A microfluidic platform to investigate the role of mechanical constraints on tissue reorganization.

by S. Tlili, F. Graner and H. Delanoë-Ayari

Supplementary Material

Supplementary Figures

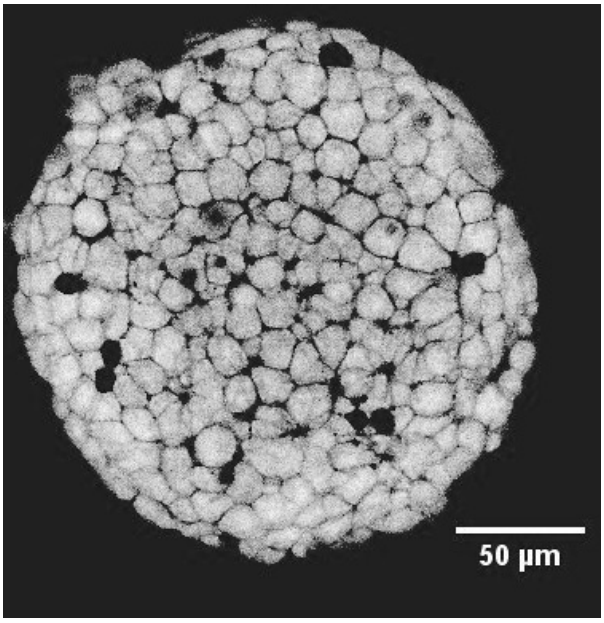

Figure 9: **F9 cell aggregate mid-section (two-photon microscopy).**

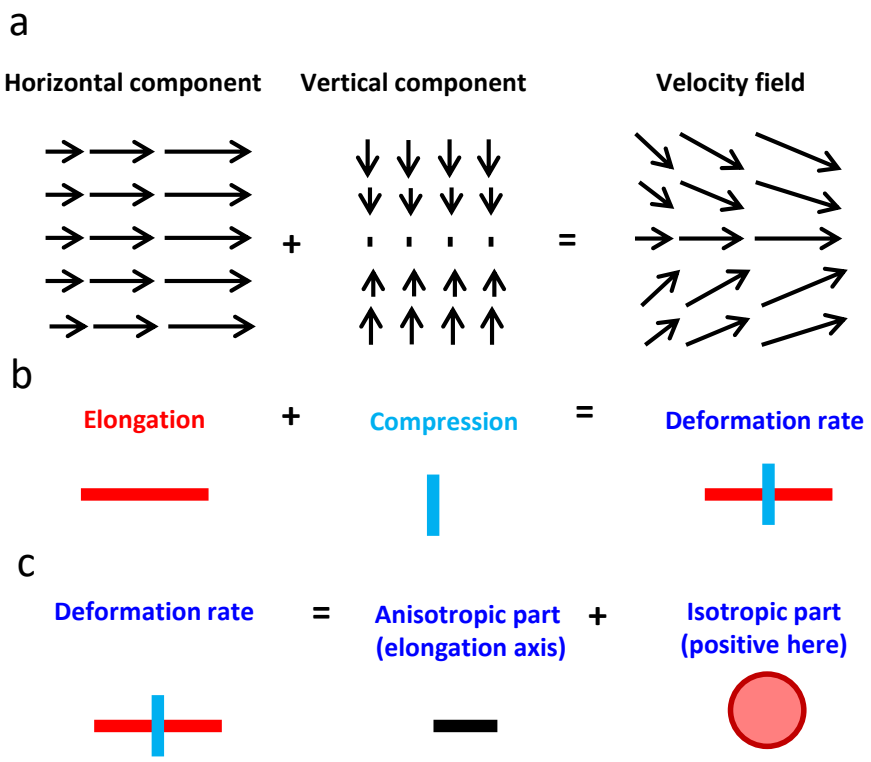

Figure 10: (a) Decomposition in horizontal and vertical components of a typical velocity field in the constriction. (b) Corresponding graphical representation of deformation rate (15). (c) Decomposition of the deformation rate in anisotropic and isotropic parts, and corresponding graphical representation (15).

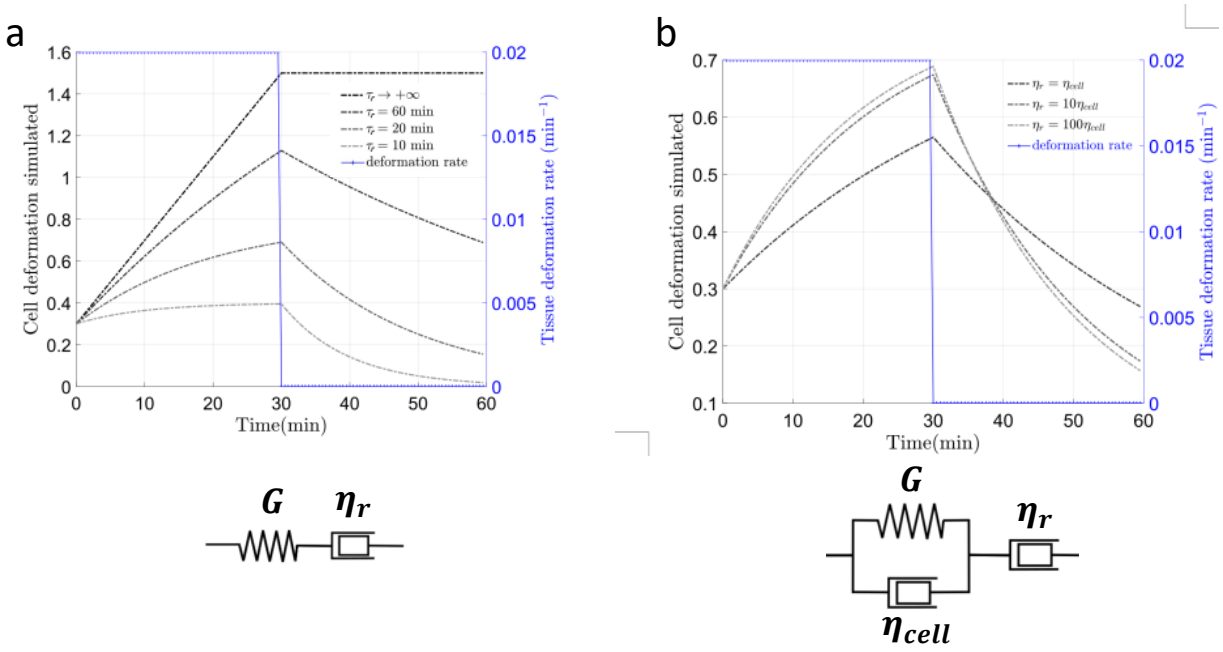

Figure 11: **Idealized mechanical responses**. Simulated time evolutions for different models (insets in a,b), τ_r values and viscosity ratios of the response to an imposed deformation rate step. Simulated equations are for (a) $\dot{\varepsilon}^{\mathrm{dev}}_{cell} = grad\ \vec{v}^{\mathrm{dev}}_{\mathrm{sym}} - \frac{\varepsilon^{\mathrm{dev}}_{cell}}{\tau_r}$ and for (b) $(1 + \frac{\eta_{cell}}{\eta_r})\dot{\varepsilon}^{\mathrm{dev}}_{cell} = grad\ \vec{v}^{\mathrm{dev}}_{\mathrm{sym}} - \frac{\varepsilon^{\mathrm{dev}}_{cell}}{\tau_r}$.

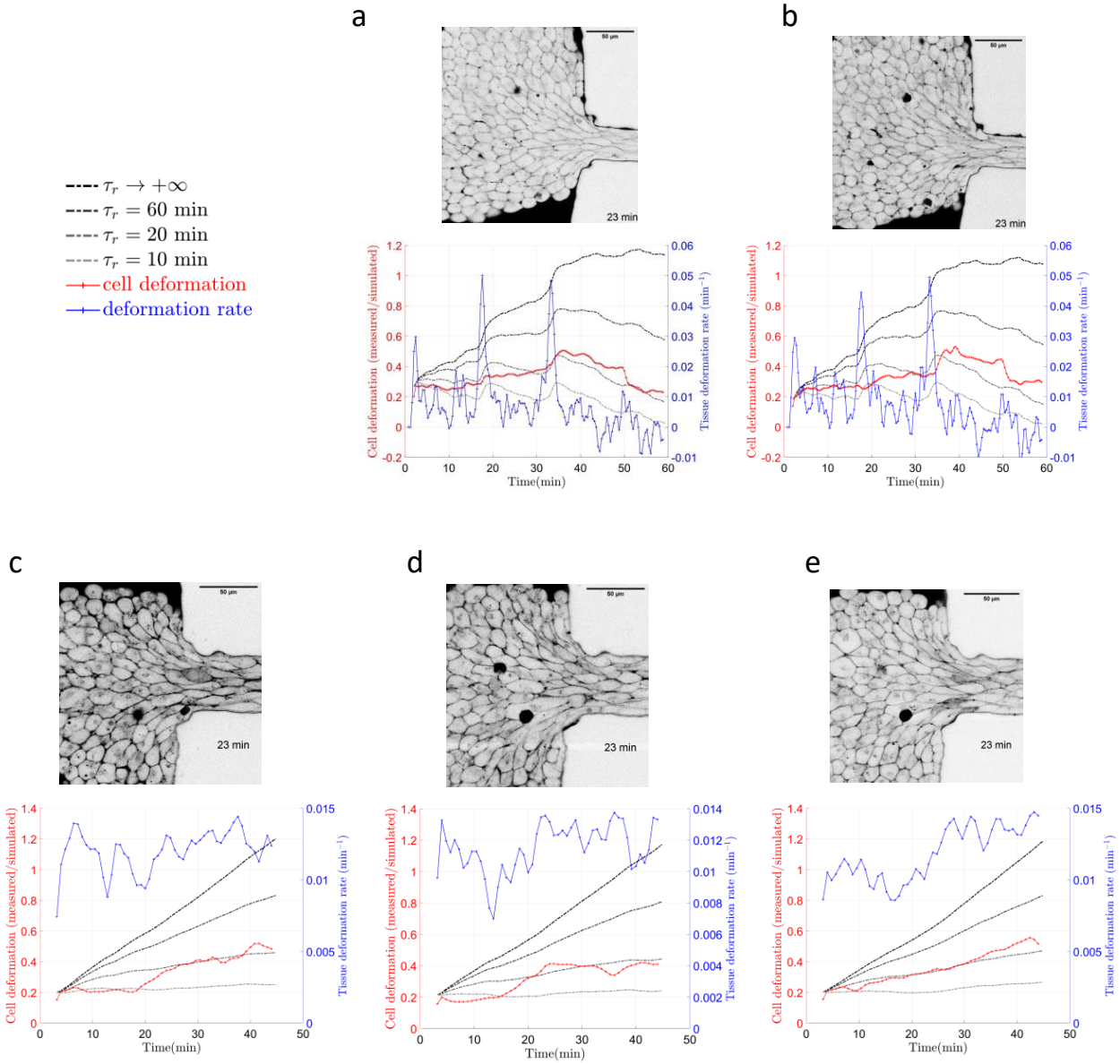

Figure 12: **Reproducibility in estimating** τ_r (same analysis and imaging methods as in Fig. 4). (a,b) Same experiment as in Fig. 4, imaged and analyzed at two different heights (Supp. Movie 14); (a) is Fig. 4c duplicated here to enable comparison taken at $z = 15$ μm from the coverslip and (b) at $z = 30$ μm from the coverslip. (c-e) Another experiment, imaged and analyzed at three different heights (Supp. Movie 15) (Heights: (c) $z = 20$ μm, (d) $z = 30$ μm and (e) $z = 40$ μm from the coverslip).

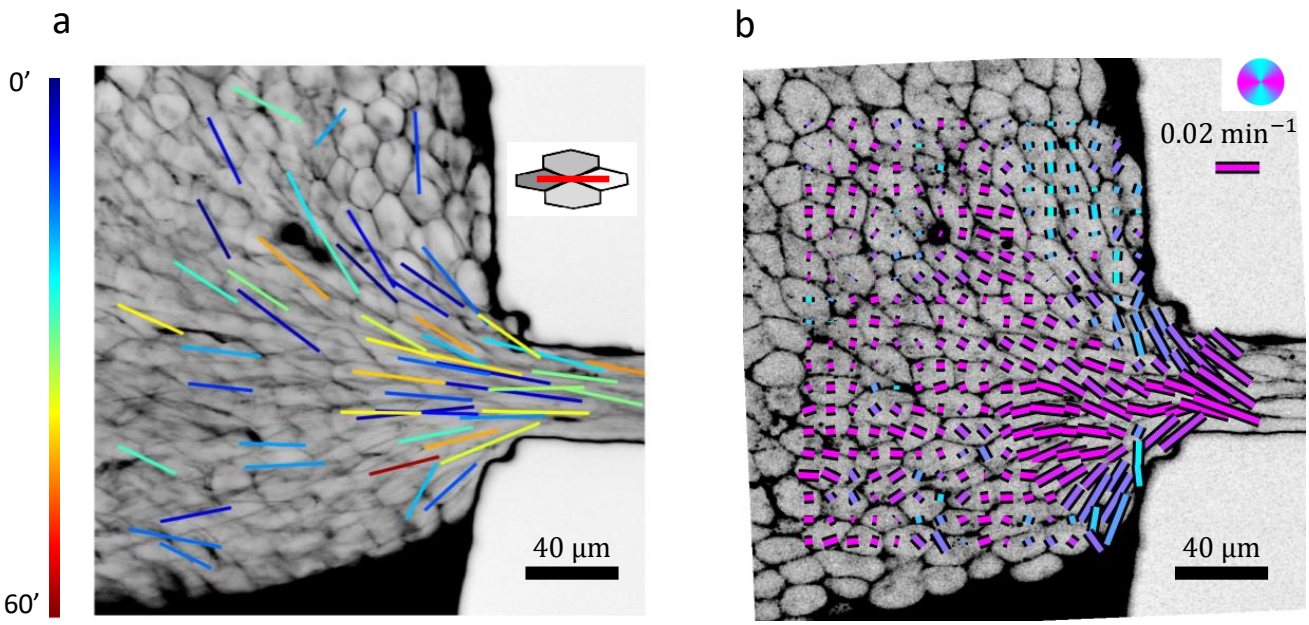

Figure 13: **Cell rearrangement map.** Rearrangements are detected in Supp. Movie 4 during one hour. (a) Position and orientation of the rearrangements detected, plotted as a bar linking both centers of cells that will lose contact just before the rearrangement (inset), and color-coded according to the timing of the four-vertex stage (in minutes). (b) Deformation rate anisotropic part averaged over time (60 minutes) with the bars color coding for their angle with respect to the channel. Zones of high rearrangements frequency correspond to high deformation rate zones.

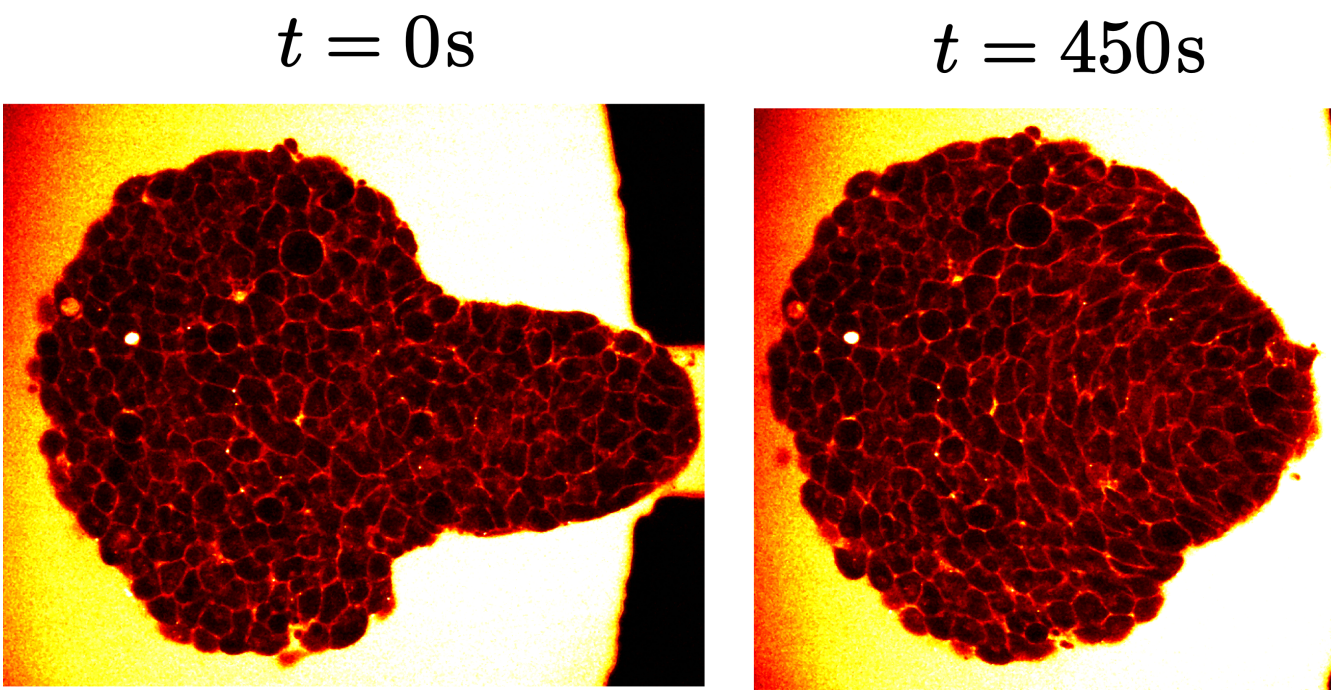

Figure 14: **Aggregate compaction after a relaxation.** An aggregate has been aspired during 1000 s. It is pushed back in the reservoir and cell shapes relax within a few seconds. Time $t = 0$ corresponds to 20 s after the pushing and cell shapes have already almost totally relaxed. After 450 s, the aggregate as a whole is round, but not each cell individually (Supp. Movie 9).

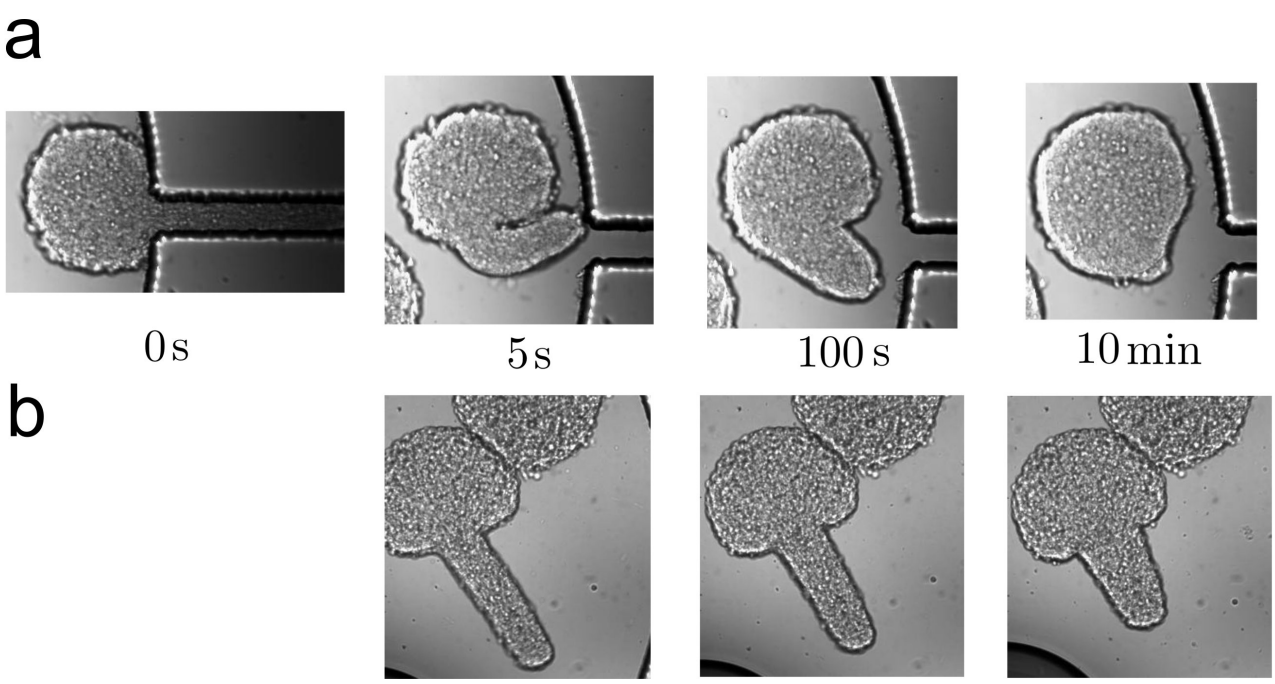

Figure 15: **First and second phases of relaxation.** (a) Brightfield image of aggregate relaxation. After a 1000 seconds long aspiration, the aggregate is left free to relax. Time $t = 0$ is counted at the end of the aspiration, *i.e.* at the beginning of the relaxation. (b) Same with 50 μM of blebbistatin to inhibit myosin II. The first fast phase of the relaxation is still present, but there is no complete return to the initial shape.

Supplementary Movies

Supplementary movies can be downloaded from the following link: https://doi.org/10.5281/zenodo.6895913

Supp. Movie 1: 40 minutes long timelapse (brightfield) of an aggregate aspired in a channel.

Supp. Movie 2: z-stack (two-photon microscopy) of a non-deformed F9 cells aggregate.

Supp. Movie 3: 60 minutes long timelapse (two-photon microscopy) of an aggregate aspired in a channel. Left: imaged plane at $z = 40$ μm from the coverslip. Middle: imaged plane in contact with the coverslip. Right: superposition of the two imaged planes.

Supp. Movie 4: 60 minutes long timelapse (two-photon microscopy) of an aggregate aspired in a channel.

Supp. Movie 5: cell-cell junctions involved in cell rearrangements in Supplementary Movie 4. Rapid relaxation rearrangements ($V^+ > 1$ μm/min) are represented in red while slow ones ($V^+ < 1$ μm/min) are in black.

Supp. Movie 6: tissue fracture appearing during a rapid aspiration (two-photon microscopy timelapse).

Supp. Movie 7: aspiration and rapid relaxation experiment (two-photon microscopy).

Supp. Movie 8: relaxation experiment after an aggregate being fully blocked in the aspiration channel during 30 minutes (two-photon microscopy).

Supp. Movie 9: relaxation experiment after a partial aspiration during which cellular deformation has relaxed (two-photon microscopy).

Supp. Movie 10: relaxation experiment after an aspiration in a short channel, with a more complex geometry during the rounding phase (two-photon microscopy).

Supp. Movie 11: other example of a relaxation experiment after an aspiration in a short channel (two-photon microscopy).

Supp. Movie 12: relaxation experiment after a partial aspiration (two-photon microscopy) in 50 μM blebbistatin medium.

Supp. Movie 13: aspiration of an α-catenin null cell line aggregate (two-photon microscopy).

Supp. Movie 14: same aspiration as in Supp. Movie 4, with two planes superimposed in red and green (heights: $z = 15$ and 30 μm from the coverslip).

Supp. Movie 15: aspiration with three planes superimposed in red, blue and green (heights: $z = 20$, 30 and 40 μm from the coverslip).